

Site-Specific X-Ray Absorption Spectroscopy of $Y_{1-x}Ca_xBa_2Cu_3O_{7-y}$: Overdoping and Role of Apical Oxygen for High Temperature Superconductivity

M. Merz,¹ N. Nücker,¹ P. Schweiss,¹ S. Schuppler,¹ C. T. Chen,² V. Chakarian,³ J. Freeland,³ Y. U. Idzerda,³
M. Kläser,⁴ G. Müller-Vogt,⁴ and Th. Wolf⁵

¹Forschungszentrum Karlsruhe, INFP, P.O. Box 3640, D-76021 Karlsruhe, Federal Republic of Germany

²Synchrotron Radiation Research Center, Hsinchu Science-based Industrial Park, Hsinchu 300, Taiwan

³Naval Research Laboratory, Code 6345, Washington, D.C. 20375

⁴Kristall- und Materiallabor, Universität Karlsruhe, D-76128 Karlsruhe, Federal Republic of Germany

⁵Forschungszentrum Karlsruhe, ITP, P.O. Box 3640, D-76021 Karlsruhe, Federal Republic of Germany

(Received 27 March 1997)

Using polarization-dependent O 1s and Cu 2p near-edge x-ray absorption spectroscopy on detwinned $Y_{1-x}Ca_xBa_2Cu_3O_{7-y}$ single crystals, the unoccupied electronic structure of the CuO_2 planes and CuO_3 chains has been studied. Unlike the conventional picture where superconductivity is related predominantly to the number of planar holes, we find clear evidence for a prominent role of the apical sites. For both under- and overdoped samples the hole states in the planes and chains are identified and hole counts for the relevant orbitals near the Fermi level are derived. Oxygen-deficient as well as oxygen-rich samples show that the holes introduced by replacing Y^{3+} with Ca^{2+} appear solely in the planes. [S0031-9007(98)06297-8]

PACS numbers: 74.25.Jb, 74.62.Dh, 74.72.Bk, 78.70.Dm

The well-known crystallographic structure of $YBa_2Cu_3O_{7-y}$ contains two-dimensional CuO_2 planes embedded between Ba and Y layers and, additionally, one-dimensional CuO_3 chains along the **b** axis of the crystal. It is widely accepted now that while the Ba^{2+} and Y^{3+} ions merely serve as counterions to stabilize the compound, the formation of the chains is responsible for the hole doping of the planes. Starting with the charge-transfer insulator $YBa_2Cu_3O_{6.0}$, the number of holes in the planes is increased by raising the oxygen content until, at $y \approx 0.6$, the compound undergoes a tetragonal to orthorhombic phase transition and superconductivity sets in [1]. For $y \approx 0.06$, the superconducting transition temperature T_c approaches its maximum value of ≈ 93 K and, finally, on increasing the oxygen content beyond 6.94, drops slightly when the threshold to overdoping is passed [2]. However, the highest oxygen content attainable is 7.0 and, consequently, the planes of $YBa_2Cu_3O_{7.0}$ are barely overdoped compared to what is possible in $La_{2-x}Sr_xCu_2O_{4+\delta}$ or $Tl_2Ba_2CuO_{6+\delta}$ [3].

Intriguingly, an alternative doping mechanism is possible by the partial replacement of Y^{3+} for divalent alkaline-earth metals such as Ca^{2+} [4]. Since the Y site is situated right between the two CuO_2 planes, one expects from this substitution that holes are mainly introduced into the planes while the charge balance of the chains remains essentially unaffected. In this sense, oxygen-deficient $Y_{1-x}Ca_xBa_2Cu_3O_{7-y}$ is unique among all *p*-type high temperature superconductors, where usually the CuO_2 planes cannot be doped without simultaneously introducing holes on the apical site or significantly changing the (chemical) pressure. In addition, the overdoped regime becomes accessible if Ca-doped samples are strongly oxygenized. From the comparison of the two

doping mechanisms conclusions about the chain unit can be expected. Especially, the correlation between the critical temperature in optimally doped high temperature superconductors T_c^{\max} and the apical hole count could be investigated. Such a relationship, if present, would greatly help in deciding whether the inclusion of next-nearest-neighbor hopping in band models is important [5].

In this paper, we report on the site-specific unoccupied electronic structure at the Fermi level E_F of $Y_{1-x}Ca_xBa_2Cu_3O_{7-y}$ as measured by O 1s and Cu 2p near edge x-ray absorption fine structure (NEXAFS). O 1s and Cu 2p NEXAFS measurements predominantly probe unoccupied O 2p and Cu 3d states, respectively. The absorption edges were obtained at the National Synchrotron Light Source (NSLS) using polarized synchrotron radiation from the NRL-NSLS beam line U4B. The measurements were performed in the nonsurface sensitive fluorescence yield mode with an energy resolution of 220 meV at 530 eV and 480 meV at 930 eV. The data were corrected for the energy-dependent incident photon flux as well as for self-absorption effects [6] and were normalized to tabulated cross sections [7] in an energy range about 70 eV above the threshold energy. Details on the correction process and on crystal growth as well as detwinning and annealing procedures are described elsewhere [8,9]. In order to characterize our samples we performed neutron diffraction experiments on single crystals from the same batches at the four-circle diffractometer 5C2 at the Orphée reactor, Laboratoire Léon Brillouin, CE Saclay [10] along with energy dispersive x-ray emission. It turns out from these data that for none of the samples does the amount of Ca incorporated on the Ba site exceed 1%.

Using the polarized character of synchrotron radiation and taking into account that the spectral region around

E_F is dominated by σ -bonded O orbitals [11], $\mathbf{E}\parallel\mathbf{a}$ contributions are caused by unoccupied O(2) $2p_x$ orbitals. Accordingly, $\mathbf{E}\parallel\mathbf{b}$ contributions result from O(3) $2p_y$ orbitals in the CuO_2 planes and, in addition, from O(1) $2p_y$ orbitals in the CuO_3 chains. By the same token, only the O(4) $2p_x$ orbitals of the two apical oxygen sites contribute for $\mathbf{E}\parallel\mathbf{c}$. Information on the unoccupied Cu(1, 2) $3d$ states in the chains and planes, respectively, can be obtained from polarization-dependent NEXAFS of the Cu $2p$ edge, although there the situation is more complicated.

In Fig. 1, the O $1s$ $\mathbf{E}\parallel\mathbf{a}$ spectra of oxygen-depleted samples ($y \approx 1.0$) with Ca concentrations of $x = 0.03, 0.12,$ and 0.23 are compared to underdoped $\text{YBa}_2\text{Cu}_3\text{O}_{6.5}$, nearly optimally doped $\text{YBa}_2\text{Cu}_3\text{O}_{6.91}$, and overdoped $\text{Y}_{0.9}\text{Ca}_{0.1}\text{Ba}_2\text{Cu}_3\text{O}_{6.91}$. For insulating $\text{Y}_{0.97}\text{Ca}_{0.03}\text{Ba}_2\text{Cu}_3\text{O}_{6.0}$ a distinct upper Hubbard band (UHB) is observed at about 530 eV [12]. With increasing Ca content the intensity of the UHB is reduced and a further peak on the low-energy side of the UHB increases. This, in turn, means that holes are created in the valence band (VB) and spectral weight is transferred from the UHB to the VB [13]. As can be seen from the comparison of $\text{Y}_{0.77}\text{Ca}_{0.23}\text{Ba}_2\text{Cu}_3\text{O}_{6.0}$ and $\text{YBa}_2\text{Cu}_3\text{O}_{6.5}$ this transfer occurs in an analogous way for the two doping mechanisms mentioned above. The intensity of the VB peak and, therefore, the number of doped holes in planar O $2p_x$ orbitals are approximately equal. When going from the underdoped through the optimally to the overdoped regime the intensity of the UHB is further reduced, and at the same time the VB intensity

is continuously increased. Because of this successive transfer of spectral weight from the UHB to the VB [12], the O- as well as the Ca-induced hole states in the planes can be identified as in-plane O $2p_\sigma$ states hybridized with Cu $3d_{x^2-y^2}$ orbitals [14], frequently referred to as Zhang-Rice (ZR) [15] states.

This picture is confirmed by the Cu $2p$ $\mathbf{E}\parallel\mathbf{a}$ data depicted in Fig. 2(a). Independent of the doping mechanism and of the number of holes introduced to the planes, an almost identical Cu^{2+} peak, ascribed to $\text{Cu } 3d^9 \rightarrow \text{Cu } 2p 3d^{10}$ transitions [14], is observed at 931.7 eV. These findings illustrate the fact that irrespective of the doping mechanism the formation of holes takes place on O rather than on Cu sites. Ca- as well as O-doped samples exhibit an additional shoulder ≈ 1.4 eV above the Cu^{2+} peak. Since this feature increases with the doping level, it corresponds to $\text{Cu } 3d^9 \underline{L} \rightarrow \text{Cu } 2p 3d^{10} \underline{L}$ transitions (\underline{L} denotes a ligand hole in an O $2p$ state) at Cu(2) $3d_{x^2-y^2}$ orbitals [11]. Hence, this shoulder is just an additional signature for the holes residing on ZR states. When comparing the Cu $2p$ data of $\text{Y}_{0.77}\text{Ca}_{0.23}\text{Ba}_2\text{Cu}_3\text{O}_{6.0}$ and $\text{YBa}_2\text{Cu}_3\text{O}_{6.5}$ it turns out that the two spectra are quite similar. Accordingly, the number of holes introduced to the planes is approximately equivalent for these two compounds, as was already shown above for the O $1s$ data. A further feature located at about 934 eV decreases with increasing O content but remains unaffected when the Ca concentration of oxygen-depleted samples is raised. Therefore, we ascribe this peak to monovalent Cu(1) states in the O(4)-Cu(1)-O(4) dumbbell (cf. Ref. [14]). Correspondingly,

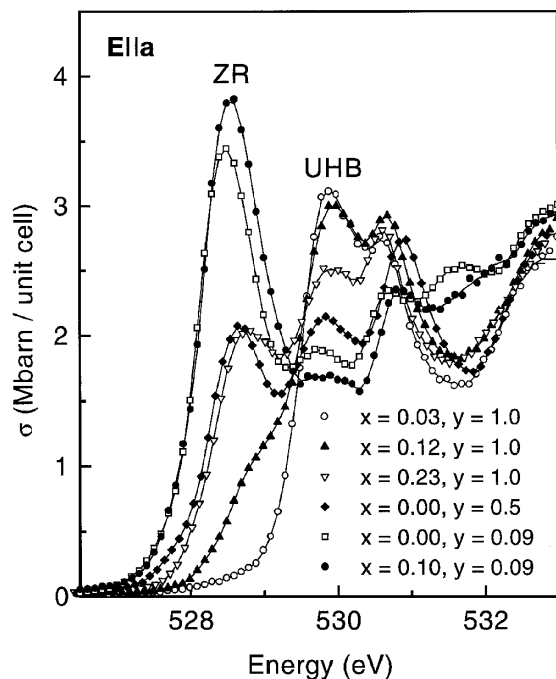


FIG. 1. Comparison of the O $1s$ $\mathbf{E}\parallel\mathbf{a}$ absorption spectra of $\text{Y}_{1-x}\text{Ca}_x\text{Ba}_2\text{Cu}_3\text{O}_{7-y}$ for various O contents, $7 - y$, and Ca concentrations, x . Upon doping, the spectral weight of the ZR state is increased at the expense of the upper Hubbard band.

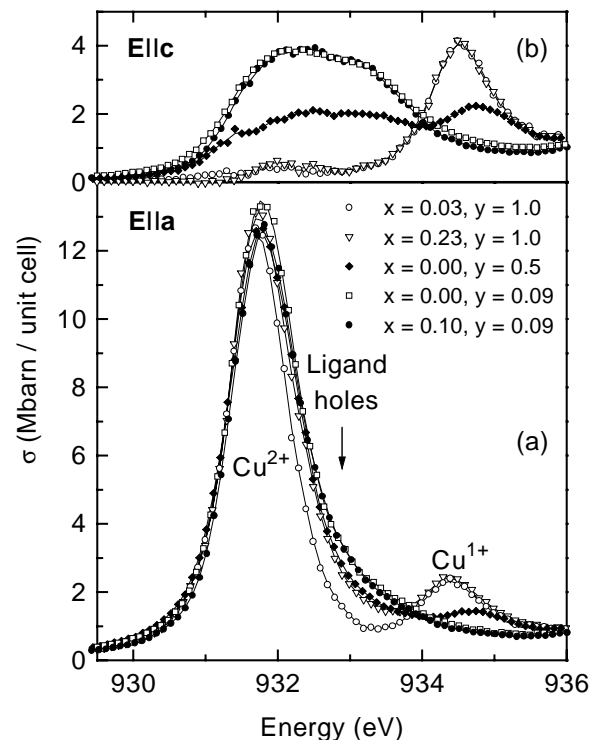


FIG. 2. Cu $2p$ absorption spectra for $\text{Y}_{1-x}\text{Ca}_x\text{Ba}_2\text{Cu}_3\text{O}_{7-y}$ for $\mathbf{E}\parallel\mathbf{a}$ (b) and $\mathbf{E}\parallel\mathbf{c}$ (a).

these monovalent states are also observed in the $\mathbf{E}\parallel\mathbf{c}$ spectra shown in Fig. 2(b). Again, a reduction of this feature with increasing O content is seen, and a broad peak centered at about 932.5 eV occurs, which arises from Cu(1) $3d_{z^2-y^2}$ and Cu(2) $3d_{3z^2-r^2}$ orbitals [16]. The two oxygen-rich samples show almost identical $\mathbf{E}\parallel\mathbf{c}$ spectra, irrespective of Ca content, indicating that none of the Ca-induced holes are transferred to these Cu orbitals.

Figure 3 shows the O $1s$ $\mathbf{E}\parallel\mathbf{c}$ spectra, assigned to the apical O(4) oxygen, while the O(1) contribution ($\mathbf{E}\parallel\mathbf{b} - \mathbf{E}\parallel\mathbf{a}$) is depicted in Fig. 4. For all Ca concentrations a distinct peak at about 531 eV is observed for the $\mathbf{E}\parallel\mathbf{c}$ spectra. This peak is assigned to transitions into the O(4)-Cu(1)-O(4) dumbbell of oxygen-depleted samples [14] and, therefore, its intensity serves as a measure of vacant O(1) sites. It is evident that this feature is reduced ($y = 0.5$) and, finally, vanishes ($y = 0.09$) with increasing O content. At the same time a broad peak at about 528 eV rises with increasing O content, implying that the formation of the chains leads to an increasing number of holes observed at the apical O(4) site. Similarly, the number of holes on O(1) sites (see Fig. 4) increases when the O content is raised. The Ca-doped but oxygen-depleted samples, however, have vacant O(1) sites (see Fig. 3), and thus neither O(1) nor O(4) contributions occur.

To further discuss the electronic structure we give estimates of the relative contributions of the O $2p_x$, O $2p_y$, and O $2p_z$ orbitals. Since the doped holes reside predominantly on O sites, as was verified above, we fix the number

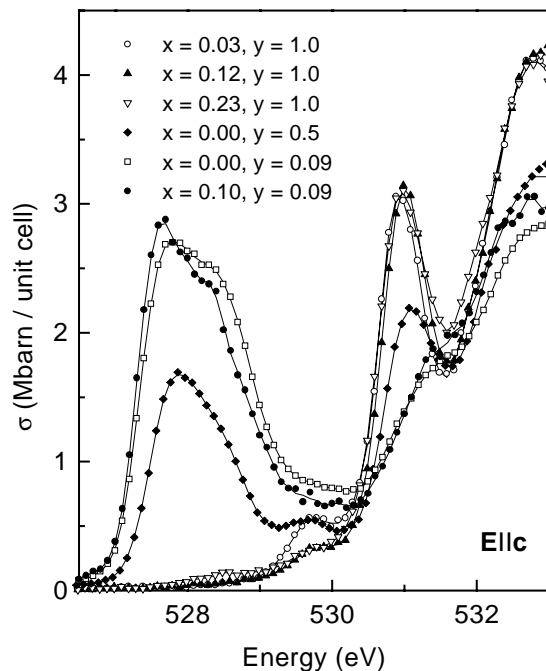


FIG. 3. $\mathbf{E}\parallel\mathbf{c}$ O $1s$ spectra of $Y_{1-x}Ca_xBa_2Cu_3O_{7-y}$. The feature at 528 eV is assigned to hole states at the apical O(4) atoms while the peak at 531 eV is a measure for vacant O(1) sites.

of introduced holes for $YBa_2Cu_3O_7$ to one. Using this scaling factor, the site-specific hole counts were derived from the integrated cross sections of the first absorption peak in the various O $1s$ spectra. For the Ca- and O-doped samples measured, the number of holes n_{plane} , n_{apex} , and n_{chain} obtained from the $\mathbf{E}\parallel\mathbf{a}$, $\mathbf{E}\parallel\mathbf{c}$, and $\mathbf{E}\parallel\mathbf{b} - \mathbf{E}\parallel\mathbf{a}$ NEXAFS data, respectively, is listed in Table I along with the T_c values. As expected, the number of planar holes increases with increasing Ca concentration and reaches 0.22 for $Y_{0.77}Ca_{0.23}Ba_2Cu_3O_{6.0}$. In agreement with optical data [17] we find the Ca-induced holes to appear solely in the planes, while none of these holes are detected on the chain unit (see also Figs. 3 and 4). This clearly contradicts a “redistribution” of holes from planes to chains presumed from ρ_c measurements [18].

Comparing the hole numbers of $YBa_2Cu_3O_{6.5}$ and $Y_{0.77}Ca_{0.23}Ba_2Cu_3O_{6.0}$, it turns out that the same amount of planar holes ($2 \times n_{\text{plane}} = 0.22$) is observed for these two compounds. The former exhibits a T_c at ≈ 55 K, whereas for the latter, remarkably, superconductivity is absent. The literature is currently divided on this issue: Older work tends to find superconductivity in similar compounds; recently, such a lack of T_c was also observed for $Y_{0.8}Ca_{0.2}Ba_2Cu_3O_{7-y}$ ($y > 0.6$) ceramics [19]. Although we cannot resolve this issue here, we find that oxygen removal in polycrystalline material under Ar flow may not be as complete as expected [20]; however, it is important to note that NEXAFS gives *direct* information on hole distributions for our samples. From Table I, it is obvious that for $YBa_2Cu_3O_{6.5}$ approximately equal amounts of holes reside on the O sites of the CuO_2 planes

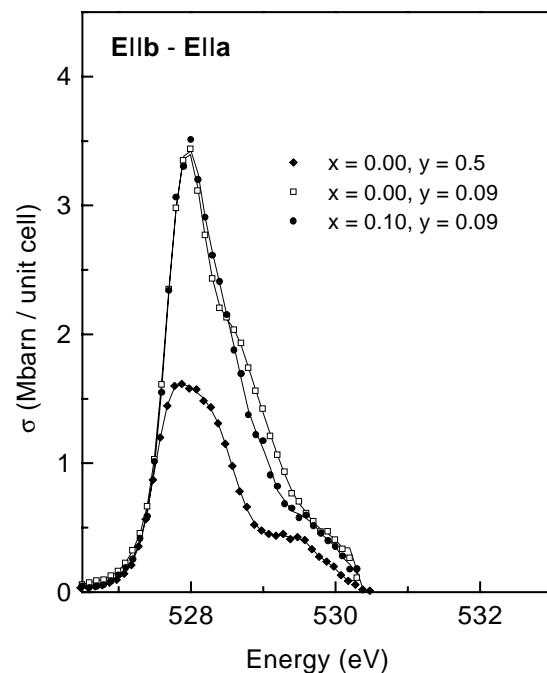


FIG. 4. Difference spectra $\mathbf{E}\parallel\mathbf{b} - \mathbf{E}\parallel\mathbf{a}$ for O-doped $YBa_2Cu_3O_{7-y}$. The spectra are ascribed to the contribution of the O(1) chain oxygen.

TABLE I. The hole distribution between the structural units of $Y_{1-x}Ca_xBa_2Cu_3O_{7-y}$. The hole numbers n_{plane} , n_{apex} , and n_{chain} are deduced from the $\mathbf{E}\|\mathbf{a}$, $\mathbf{E}\|\mathbf{c}$, and $\mathbf{E}\|\mathbf{b} - \mathbf{E}\|\mathbf{a}$ NEXAFS data. Estimated error limit for the total n : ± 0.03 .

	$2 \cdot n_{\text{plane}}$	n_{apex}	n_{chain}	T_c (K)
$Y_{0.97}Ca_{0.03}Ba_2Cu_3O_{6.0}$	0.00	0.00	0.00	0 (<4.2)
$Y_{0.88}Ca_{0.12}Ba_2Cu_3O_{6.0}$	0.10	0.00	0.00	0 (<4.2)
$Y_{0.77}Ca_{0.23}Ba_2Cu_3O_{6.0}$	0.22	0.00	0.00	0 (<4.2)
$YBa_2Cu_3O_{6.5}$	0.22	0.13	0.12	55
$YBa_2Cu_3O_{6.91}$	0.40	0.27	0.24	92
$Y_{0.9}Ca_{0.1}Ba_2Cu_3O_{6.91}$	0.49	0.26	0.23	78

and the CuO_3 chain, while for $Y_{0.77}Ca_{0.23}Ba_2Cu_3O_{6.0}$ the holes are found exclusively on the planar O(2,3) sites. This leads to an important result: Superconductivity, at least in $Y_{1-x}Ca_xBa_2Cu_3O_{7-y}$, appears only if holes reside on the chain unit, especially on the apical O(4) sites. In other words, the absence of holes on the apical sites is detrimental to high-temperature superconductivity (HTSC), independent of the number of holes introduced to the planes. Since for hole-doped materials HTSC occurs usually in compounds which contain layers including apical sites, this conclusion may be more general.

In order to investigate the effect of Ca doping on oxygenized $YBa_2Cu_3O_{7-y}$, we compare nonsubstituted $YBa_2Cu_3O_{6.91}$ with $Y_{0.9}Ca_{0.1}Ba_2Cu_3O_{6.91}$. Again, the figures and Table I show that Ca doping increases the number of holes exclusively for planar O $2p_\sigma$ orbitals, while all other orbitals remain essentially unaffected. Thus, consistent with the findings for the oxygen-depleted samples discussed above, a Ca-induced charge redistribution between the planes and the chain can be ruled out for the oxygen-rich samples also. Despite the increase of holes found for planar O $2p_\sigma$ orbitals, however, T_c drops from 92 to 78 K when going from $YBa_2Cu_3O_{6.91}$ to $Y_{0.9}Ca_{0.1}Ba_2Cu_3O_{6.91}$. One can relate this to a substantial overdoping of the planes of $Y_{0.9}Ca_{0.1}Ba_2Cu_3O_{6.91}$.

In summary, we draw the following conclusions for HTSC in $Y_{1-x}Ca_xBa_2Cu_3O_{7-y}$: Ca doping of $YBa_2Cu_3O_{7-y}$ introduces holes exclusively in the CuO_2 planes, without affecting the CuO_3 chains at all. Moreover, Ca-doped but oxygen-depleted samples exhibit no superconductivity, independent of the total hole count of the planes. On the other hand, raising the O content provokes an increase of holes at both the O(1) and the apical O(4) site which renders the sample superconducting. Therefore, to obtain the maximum achievable T_c^{max} it is not sufficient to merely have optimally doped planes; rather, an optimum hole count on the apical site is equally important. This intriguing result also offers an explanation for the somewhat unexpected decrease of T_c^{max} with increasing Ca concentration reported for samples with optimally doped planes [21]: In order to retain the optimum number of planar holes, Ca doping has to be counterbalanced by an appropriately smaller O content, thus reducing both the hole count on the apical oxygen

and T_c^{max} significantly. If the apical hole count, however, is raised by an increase of the O content, the CuO_2 planes become overdoped and T_c is lowered. In other words, in Ca-doped samples the apical site does not reach its most favorable doping level until the planes are already overdoped. Taken together, this strongly indicates that T_c^{max} in hole-doped high temperature superconductors scales not only with the planar hole concentration but is also governed by the number of holes on the apical site.

We greatly appreciate the experimental help of B. Obst, E. Sohmen, R. Neudert, J.-H. Park, S.L. Hulbert, G. Roth, D. Ernst, and B. Scheerer. The NSLS is part of Brookhaven National Laboratory, which is funded by the U.S. DOE. V.C. was supported by the Office of Naval Research.

- [1] D.C. Johnston *et al.*, *Physica* (Amsterdam) **153C-155C**, 572 (1988).
- [2] V. Breit *et al.*, *Phys. Rev. B* **52**, R15 727 (1995).
- [3] J.B. Torrance *et al.*, *Phys. Rev. Lett.* **61**, 1127 (1988); Y. Kubo *et al.*, *Phys. Rev. B* **43**, 7875 (1991).
- [4] Y. Tokura *et al.*, *Phys. Rev. B* **38**, 7156 (1988).
- [5] L.F. Feiner *et al.*, *Phys. Rev. Lett.* **76**, 4939 (1996); R. Raimondi *et al.*, *Phys. Rev. B* **53**, 8774 (1996); C. Di Castro *et al.*, *Phys. Rev. Lett.* **66**, 3209 (1991); C. Lubritto *et al.*, *J. Phys. Condens. Matter* **8**, 11 053 (1996); Y. Ohta *et al.*, *Phys. Rev. B* **43**, 2968 (1991).
- [6] L. Tröger *et al.*, *Phys. Rev. B* **46**, 3283 (1992); S. Eisebitt *et al.*, *Phys. Rev. B* **47**, 14 103 (1993).
- [7] J.J. Yeh and I. Lindau, *At. Data Nucl. Data Tables* **32**, 1 (1985); W.J. Veigele, *Handbook of Spectroscopy* (CRC Press, Cleveland, 1974), Vol. 1, p. 28.
- [8] M. Merz *et al.*, *Phys. Rev. B* **55**, 9160 (1997).
- [9] Th. Wolf *et al.*, *J. Cryst. Growth* **96**, 1010 (1989); A. Zibold *et al.*, *Physica* (Amsterdam) **171C**, 151 (1990).
- [10] Laboratoire Commun CEA-CNRS.
- [11] N. Nücker *et al.*, *Phys. Rev. B* **39**, 6619 (1989).
- [12] The UHB, although it is a Cu $3d$ on-site correlation effect, can be observed in O $1s$ x-ray absorption spectroscopy because of substantial Cu $3d_{x^2-y^2}-O 2p_{x,y}$ hybridization [14].
- [13] J. Zaanen *et al.*, *Phys. Rev. Lett.* **55**, 418 (1985); H. Eskes and G.A. Sawatzky, *Phys. Rev. Lett.* **61**, 1415 (1988).
- [14] J. Fink *et al.*, *J. Electron Spectrosc. Relat. Phenom.* **66**, 395 (1994).
- [15] F.C. Zhang and T.M. Rice, *Phys. Rev. B* **37**, 3759 (1988).
- [16] N. Nücker *et al.*, *Phys. Rev. B* **51**, 8529 (1995).
- [17] K. Widder *et al.*, *Physica* (Amsterdam) **267C**, 254 (1996).
- [18] T. Zenner *et al.*, *J. Low Temp. Phys.* **105**, 909 (1996).
- [19] J. Hejtmánek *et al.*, *Phys. Rev. B* **54**, 16 226 (1996).
- [20] Annealing $Y_{0.8}Ca_{0.2}Ba_2Cu_3O_{7-y}$ powder at 650 °C for 160 h in Ar flow resulted in $T_c = 45$ K; after subsequent annealing at $p < 10^{-8}$ mbar, no superconductivity occurred.
- [21] C. Bernhard and J.L. Tallon, *Phys. Rev. B* **54**, 10 201 (1996); J.L. Tallon *et al.*, *Phys. Rev. B* **51**, 12 911 (1995).